JCB Article

# Smn, the spinal muscular atrophy–determining gene product, modulates axon growth and localization of β-actin mRNA in growth cones of motoneurons

**Wilfried Rossoll,[1] Sibylle Jablonka,[1] Catia Andreassi,[1] Ann-Kathrin Kröning,[1] Kathrin Karle,[1] Umrao R. Monani,[2] and Michael Sendtner[1]**

[1]Institute for Clinical Neurobiology, University of Wuerzburg, 97080 Wuerzburg, Germany
[2]Department of Molecular and Cellular Biochemistry, The Ohio State University, Columbus, OH 43210

Spinal muscular atrophy (SMA), a common autosomal recessive form of motoneuron disease in infants and young adults, is caused by mutations in the survival motoneuron 1 (*SMN1*) gene. The corresponding gene product is part of a multiprotein complex involved in the assembly of spliceosomal small nuclear ribonucleoprotein complexes. It is still not understood why reduced levels of the ubiquitously expressed SMN protein specifically cause motoneuron degeneration. Here, we show that motoneurons isolated from an SMA mouse model exhibit normal survival, but reduced axon growth. Overexpression of Smn or its binding partner, heterogeneous nuclear ribonucleoprotein (hnRNP) R, promotes neurite growth in differentiating PC12 cells. Reduced axon growth in Smn-deficient motoneurons correlates with reduced β-actin protein and mRNA staining in distal axons and growth cones. We also show that hnRNP R associates with the 3′ UTR of β-actin mRNA. Together, these data suggest that a complex of Smn with its binding partner hnRNP R interacts with β-actin mRNA and translocates to axons and growth cones of motoneurons.

## Introduction

Spinal muscular atrophy (SMA) represents one of the most common genetic diseases leading to death in childhood. It is caused by homozygous mutations or loss of the telomeric copy of the survival motoneuron (*SMN*) gene on human chromosome 5q13 (Lefebvre et al., 1995). The human *SMN* gene is located within a duplicated chromosomal region, and both *SMN* genes are expressed. They differ in that the telomeric copy (*SMN1*) expresses primarily a full-length transcript, whereas the centromeric *SMN* gene (*SMN2*) expresses primarily a truncated isoform (Lorson et al., 1999; Monani et al., 1999). The truncated transcript lacks exon 7, which encodes the most COOH-terminal 16 residues, and this protein appears unable to compensate for *SMN1* deficiency in SMA. Mice contain only one copy of *Smn*, and its homozygous disruption leads to massive cell death during early embryonic development (Schrank et al., 1997). In mouse models with reduced *Smn* gene dose (Frugier et al., 2000; Hsieh-Li et al., 2000; Jablonka et al., 2000) or in which human *SMN2* is expressed at low levels on an *Smn*-null background (Monani et al., 2000, 2003), motoneuron degeneration and an SMA-like phenotype are observed.

SMN plays an essential role in assembly and regeneration of spliceosomal small nuclear ribonucleoproteins (snRNPs) in all cell types (Fischer et al., 1997; Meister et al., 2002; Paushkin et al., 2002). Despite progress in the understanding of the function of SMN in these processes, very little is known about the cause of the mainly motoneuron-specific pathology in SMA. There is no evidence that abnormalities of spliceosomal snRNP biogenesis and metabolism cause defects in mRNA splicing in motoneurons from mouse models (Jablonka et al., 2000) or SMA patients (for review see Sendtner, 2001).

Several lines of evidence support additional neuron-specific functions of SMN. Mice in which the *Smn* gene is specifically deleted in neurons show postnatal cell death (Frugier et al., 2000) associated with accumulation of neurofilament in motoneuron cell bodies and at the motor endplate

W. Rossoll and S. Jablonka contributed equally to this paper.

The online version of this article includes supplemental material.

Address correspondence to Michael Sendtner, Institute for Clinical Neurobiology, Josef-Schneider-Str. 11, 97080 Wuerzburg, Germany. Tel.: (49) 931-201-49767. Fax: (49) 931-201-49788.
email: sendtner@mail.uni-wuerzburg.de

Key words: SMA; SMN; RNA transport; β-actin; hnRNP R

Abbreviations used in this paper: hnRNP, heterogeneous nuclear ribonucleoprotein; phospho-tau, phosphorylated tau protein; RRM, RNA recognition motif; SMA, spinal muscular atrophy; SMN, survival motoneuron; snRNPs, small nuclear ribonucleoproteins.

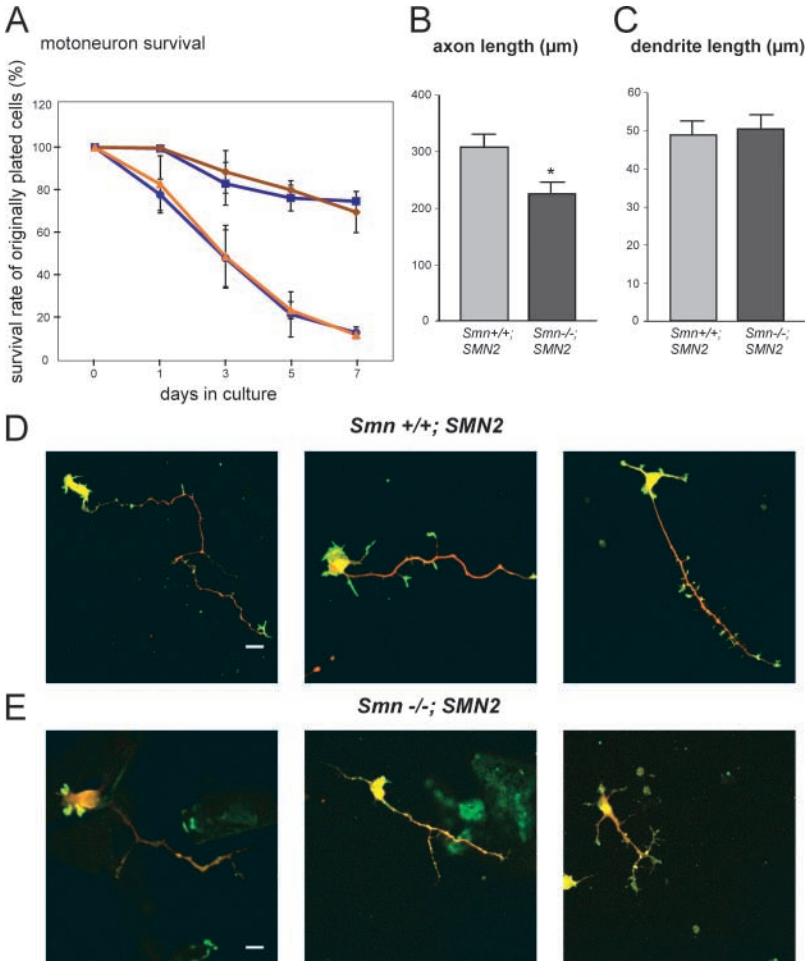


Figure 1. **Survival and neurite outgrowth of primary cultured motoneurons from *Smn*$^{+/+}$; *SMN2* and *Smn*$^{-/-}$; *SMN2* mice.** (A) Survival (percentage of originally plated cells) of *Smn*$^{+/+}$; *SMN2* (blue) and *Smn*$^{-/-}$; *SMN2* (orange) motoneurons in the presence (squares) or absence (triangles/circles) of ciliary neurotrophic factor and brain-derived neurotrophic factor. Motoneurons were cultured for 7 d, and survival was scored every 2 d ($n = 3$). Average length of longest axonal branches (B) and dendritic processes (C) of motoneurons after 5 d in culture is shown. Motoneurons from *Smn*$^{-/-}$; *SMN2* mice exhibit a significant reduction in axon length (224.7 ± 20.5 μm vs. 307.6 ± 23.1 μm), whereas dendrite length was not affected. Asterisk denotes significant differences ($P < 0.05$; $n = 4$). (D and E) Immunostaining of fixed cells with antibodies against MAP-2 protein (green processes) and axon-specific phospho-tau protein (red processes). Typical examples are shown for *Smn*$^{+/+}$; *SMN2* (D) and *Smn*$^{-/-}$; *SMN2* (E) motoneurons. Bar, 20 μm.

(Cifuentes-Diaz et al., 2002). The Smn protein is localized in axons and growth cones of motoneurons, both in cell culture and in vivo (Jablonka et al., 2001; Fan and Simard, 2002). Interestingly, Smn is not colocalized with Gemin2 in axons (Jablonka et al., 2001). Because Gemin2 is an essential component of complexes that assemble snRNPs, this finding suggests that Smn might serve additional functions in axons of motoneurons. Two novel interaction partners for Smn, the highly related RNA-binding heterogeneous nuclear ribonucleoproteins R and Q (hnRNP R and hnRNP Q, respectively; Mourelatos et al., 2001), have been found to colocalize with Smn in motor axons (Rossoll et al., 2002).

Here, we report that Smn and its binding partner hnRNP R modulate axon growth. We measured survival and neurite length in isolated motoneurons from a mouse model of SMA and found a specific reduction in axon growth, but no alterations in survival or dendrite length. Moreover, neurite outgrowth is enhanced in PC12 cells overexpressing Smn and/or hnRNP R. We also show that deficiency of Smn protein leads to alterations of β-actin protein and mRNA localization in axons and growth cones. hnRNP R associates with β-actin mRNA, and binding of Smn to hnRNP R appears necessary for this interaction. These data indicate that Smn and hnRNP R are involved in processing and localization of β-actin mRNA to growth cones of developing motoneurons. A defect in this function could explain the relatively high specificity of the disease for motoneurons.

## Results

### Reduced axon growth in Smn-deficient motoneurons

Primary motoneurons were isolated from the lumbar spinal cord of control and *Smn*$^{-/-}$; *SMN2* mouse embryos that carry two copies of the *SMN2* transgene (Monani et al., 2000). These mice die shortly after birth by muscle paralysis and motoneuron degeneration, and thus serve as a mouse model for the most severe form of SMA. Ciliary neurotrophic factor and brain-derived neurotrophic factor were added as survival factors during culture periods of at least 5 d. The number of surviving motoneurons was determined every second day. No differences were observed between *Smn*$^{+/+}$; *SMN2* and *Smn*$^{-/-}$; *SMN2* motoneurons at any time point investigated (Fig. 1 A).

To measure neurite length, motoneurons were fixed after 5 d in culture and immunostained with antibodies against the microtubule-associated proteins MAP-2 and phosphorylated tau protein (phospho-tau) for identification of dendritic and axonal processes. Phospho-tau–stained axonal processes were significantly shorter (27%) in *Smn*$^{-/-}$; *SMN2* motoneurons (224.7 ± 20.5 μm vs. 307.6 ± 23.1 μm), whereas dendrite outgrowth was not altered (Fig. 1, B–E). These results indicate that axon growth (but not sur-

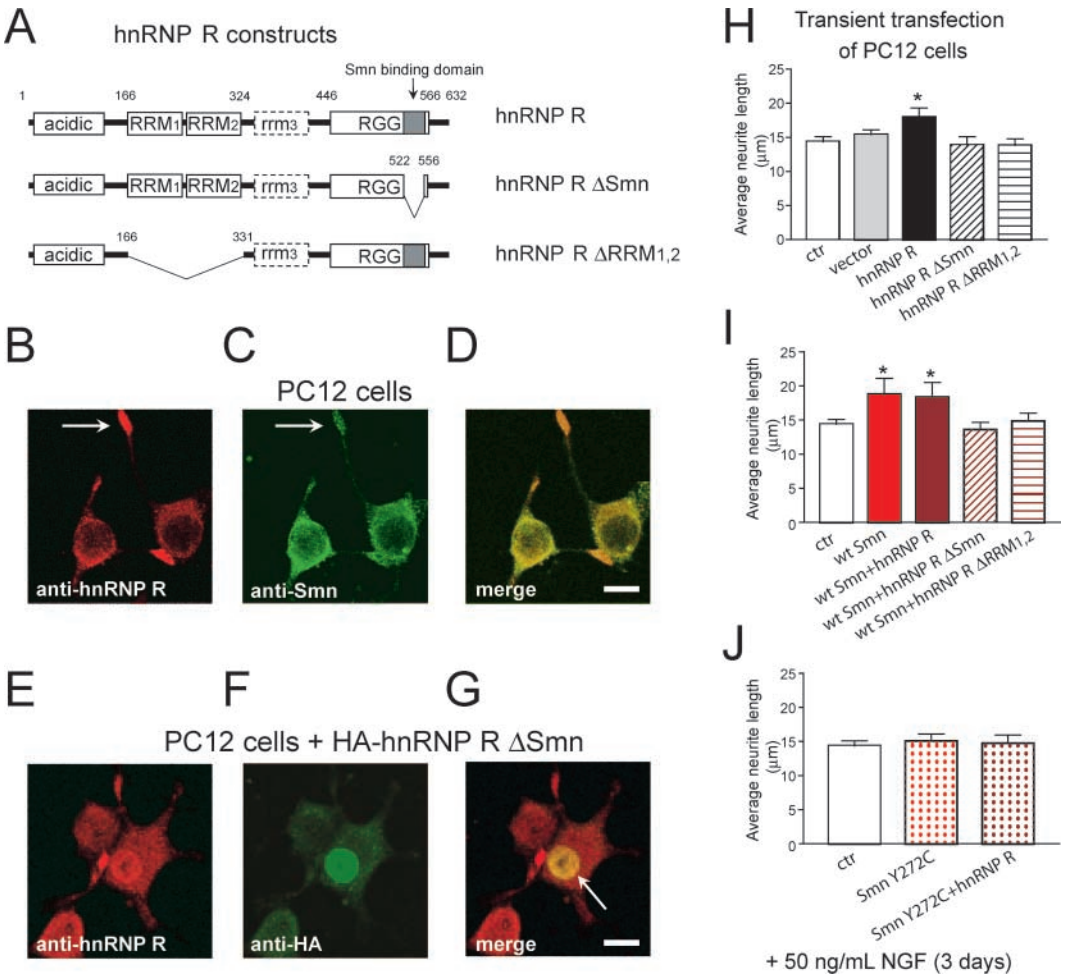


Figure 2. **hnRNP R overexpression increases neurite outgrowth.** (A) Schematic representation of the domain structure of wild-type hnRNP R and mutants used to transfect PC12 cells. Either the Smn-binding domain (hnRNP R ΔSmn) or the RNA recognition motifs 1 and 2 (hnRNP R ΔRRM1,2) were deleted. Acidic, protein domain rich in acidic amino acids; RRM, RNA recognition motif; RGG, arginine-glycine-glycine–rich domain. The dashed box indicates a potential additional RRM. Numbers refer to amino acids. (B) PC12 cells were allowed to differentiate for 3 d with NGF, and were then stained with anti-hnRNP R. Intense labeling of growth cones (arrow) and a punctuate nuclear and cytoplasmic staining was observed. (C) anti-Smn staining shows a strong nuclear signal in gem-like structures and a diffuse signal in the cytoplasm and neural processes, including growth cones (arrow). (D) A merge of B and C shows partial colocalization of hnRNP R and Smn in the cell body and colocalization at the growth cones. Bar, 10 μm. In contrast to the endogenous protein (cytoplasmic staining in E and G), most of the HA-tagged protein lacking the Smn-binding domain is localized to the nucleus (nuclear staining in E–G; arrow in G). Bar, 10 μm. After differentiation for 3 d with NGF (H), cells transfected with wild-type hnRNP R show a 25% increase in neurite length (measured as described in the Materials and methods section), whereas overexpression of mutant constructs had no effect on neurite length. (I) Overexpression of wild-type Smn also leads to an increase in neurite extension (~30%), but cotransfection of wild-type Smn and hnRNP R had no additive effect on neurite extension. Overexpression of mutant hnRNP R with wild-type Smn (I) or mutant SmnY272C with wild-type hnRNP R (J) suppressed the stimulation of neurite outgrowth. Results represent the mean ± SEM of pooled data from four independent transient transfection experiments (H–J). *, $P < 0.05$ compared with control cells by *t* test. Only transfected cells as identified by staining with the HA antibody (hnRNP R constructs) or FLAG antibody (Smn constructs) were scored.

vival) is specifically reduced in motoneurons from an animal model of SMA.

## Smn and hnRNP R promote neurite growth in PC12 cells

Because reduced Smn protein levels lead to reduced axonal growth, we examined whether overexpression of Smn or its binding partner hnRNP R affects neurite outgrowth in differentiating neuronal cells. For this purpose, we transiently transfected PC12 cells with expression constructs for wild-type and mutant Smn as well as the Smn-interacting protein hnRNP R. We also tested hnRNP R mutants lacking the Smn interaction domain, which has been identified between aa 522 and 556 (hnRNP R ΔSmn; Mourelatos et al., 2001). Because hnRNP R, in contrast to Smn, contains RNA-binding domains, we also tested mutants lacking the RNA recognition motifs (RRM) 1 and 2 between aa 166 and 331 (Fig. 2 A; hnRNP R ΔRRM1,2). RRM1 and RRM2 appear to be the primary RNA-binding sites (Rossoll et al., 2002). The Smn interaction domain is highly homologous between hnRNP R and the closely related hnRNP Q (Mourelatos et al., 2001). Endogenous protein was detected with anti-hnRNP R antibody, whereas overexpressed wild-type or truncated hnRNP R forms were identified with an mAb against the $NH_2$-terminal HA tag, but also with hnRNP R

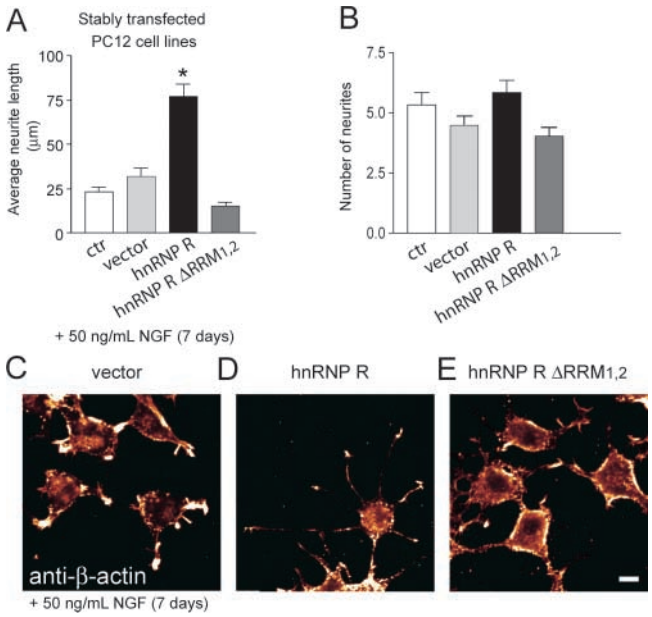


Figure 3. **hnRNP R–overexpressing cell lines exhibit increased neurite outgrowth, whereas hnRNP R ΔRRM1,2 expression leads to reduced β-actin in growth cones.** (A) PC12 cell lines overexpressing the indicated constructs were treated for 7 d with NGF. In hnRNP R–overexpressing cell lines, neurite length was increased 2.4-fold (measured as described in the Materials and methods section). (B) The number of neurites was not significantly altered. (C–E) β-Actin immunostaining shows a distinct signal in growth cones of control cell lines (C). hnRNP R–overexpressing cell lines exhibit strong staining in growth cones, which correlates with enhanced neurite growth (D). In hnRNP R ΔRRM1,2–expressing clones (E), β-actin staining was reduced in growth cones and apparently concentrated within cell bodies. In these cells, neurite growth was low. Bar, 10 μm. Results represent the mean ± SEM of pooled data from three different stable cell lines (A and B). *, $P < 0.05$ between overexpressing cell lines and controls.

antibodies as a control. As observed previously with primary cultured motoneurons, wild-type hnRNP R colocalized with Smn in cell bodies and neuritic processes of differentiating PC12 cells (Fig. 2, B–D). In contrast, HA-tagged hnRNP R ΔSmn was present mainly in the nucleus (Fig. 2, E–G). This finding suggests that interaction with Smn influences the subcellular distribution of hnRNP R. No gross mislocalization of Smn was detectable in cell lines overexpressing hnRNP R constructs (Fig. S1, available at http://www.jcb.org/cgi/content/full/jcb.200304128/DC1).

Next, we examined whether Smn or its binding partner hnRNP R modulate neurite outgrowth in PC12 cells. Transiently transfected cells overexpressing full-length hnRNP R show a 25–30% increase in neurite length after differentiation for 3 d in the presence of NGF, whereas hnRNP R mutants lacking either the RRMs (hnRNP R ΔRRM1,2) or the putative Smn interaction domain (hnRNP R ΔSmn) have no effect (Fig. 2 H). Overexpression of full-length Smn has a similar effect on neurite outgrowth, as does hnRNP R. This effect is not enhanced by co-overexpression of hnRNP R, but it is suppressed by co-overexpression of the truncated hnRNP R constructs (Fig. 2 I). Similarly, co-overexpression of a mutant Smn (SmnY272C) that is associated with severe motoneuron disease (Rochette et al., 1997) suppresses the positive effect of full-length hnRNP R (Fig. 2 J). These differences in neurite growth were even more pronounced in stably transfected PC12 cell lines overexpressing either wild-type hnRNP R or hnRNP R ΔRRM1,2. Wild-type hnRNP R (but not the truncated form) enhanced neurite length more than three times after 7 d of treatment with NGF (Fig. 3 A). As a control, we determined whether hnRNP R overexpression alters the number of neurites, but did not observe significant effects (Fig. 3 B). Similar results were observed with cell lines overexpressing full-length hnRNP Q (unpublished data).

## hnRNP R modulates β-actin content in growth cones

Reduced axon growth is observed in a variety of motoneuron disorders, and defects in a guanine nucleotide exchange factor (ALS2; Hadano et al., 2001; Yang et al., 2001), defective microtubule assembly (Tbce; Bommel et al., 2002; Martin et al., 2002), and disturbances in axonal transport (KIF1A; Yonekawa et al., 1998) have been identified as the cellular basis underlying the various forms of the disease. Actin is predominantly localized in growth cones and plays a major role in growth cone movements and neurite growth. Morphological inspection of cultured motoneurons from *Smn*$^{-/-}$*; SMN2* mice suggested a specific atrophy of growth cones when compared with control motoneurons. Therefore, we investigated the distribution of β-actin in PC12 cells and primary motoneurons. NGF-treated PC12 cell lines were immunostained with a β-actin mAb. β-Actin staining was highly concentrated in growth cones of mock-transfected and wild-type hnRNP R–overexpressing cell lines, but not in hnRNP R ΔRRM1,2–overexpressing PC12 cells (Fig. 3, C–E). This dominant-negative effect suggests that functional hnRNP R is required for localization of β-actin in growth cones.

## Reduced hnRNP R and β-actin in Smn-deficient motor axons

Previous EM analyses showed that Smn protein is associated with axonal microtubules (Bechade et al., 1999; Pagliardini et al., 2000). We have found that Smn protein is colocalized with the RNA-binding protein hnRNP R (Rossoll et al., 2002), but not with Gemin2 in motor axons (Jablonka et al., 2001), indicating that a complex of Smn and hnRNP R might be involved in axonal RNA transport or processing (Rossoll et al., 2002). Therefore, we investigated whether distribution of β-actin is disturbed in motoneurons from *Smn*$^{-/-}$*; SMN2* mice. In wild-type motoneurons, β-actin staining was concentrated in distal parts of the axon (Fig. 4 A). In axons of *Smn*$^{-/-}$*; SMN2* motoneurons, β-actin staining was very faint in growth cones and distal parts of the axon (Fig. 4 B). The isoform-specific antibody used for visualization of β-actin recognizes the $NH_2$ terminus (aa 2–15), and this epitope could be masked by posttranslational modification or actin-binding proteins. Therefore, we also performed immunostaining with anti-actin antibodies that recognize a more COOH-terminal epitope (aa 50–70). Again, disturbed distribution of actin was found in the distal axon and growth cone of motoneurons isolated from *Smn*$^{-/-}$*; SMN2* embryos (Fig. 4 D).

To examine the distribution of hnRNP R, we stained isolated motoneurons from *Smn*$^{+/+}$*; SMN2* and *Smn*$^{-/-}$*; SMN2* mice with anti-hnRNP R antibodies. Punctuate

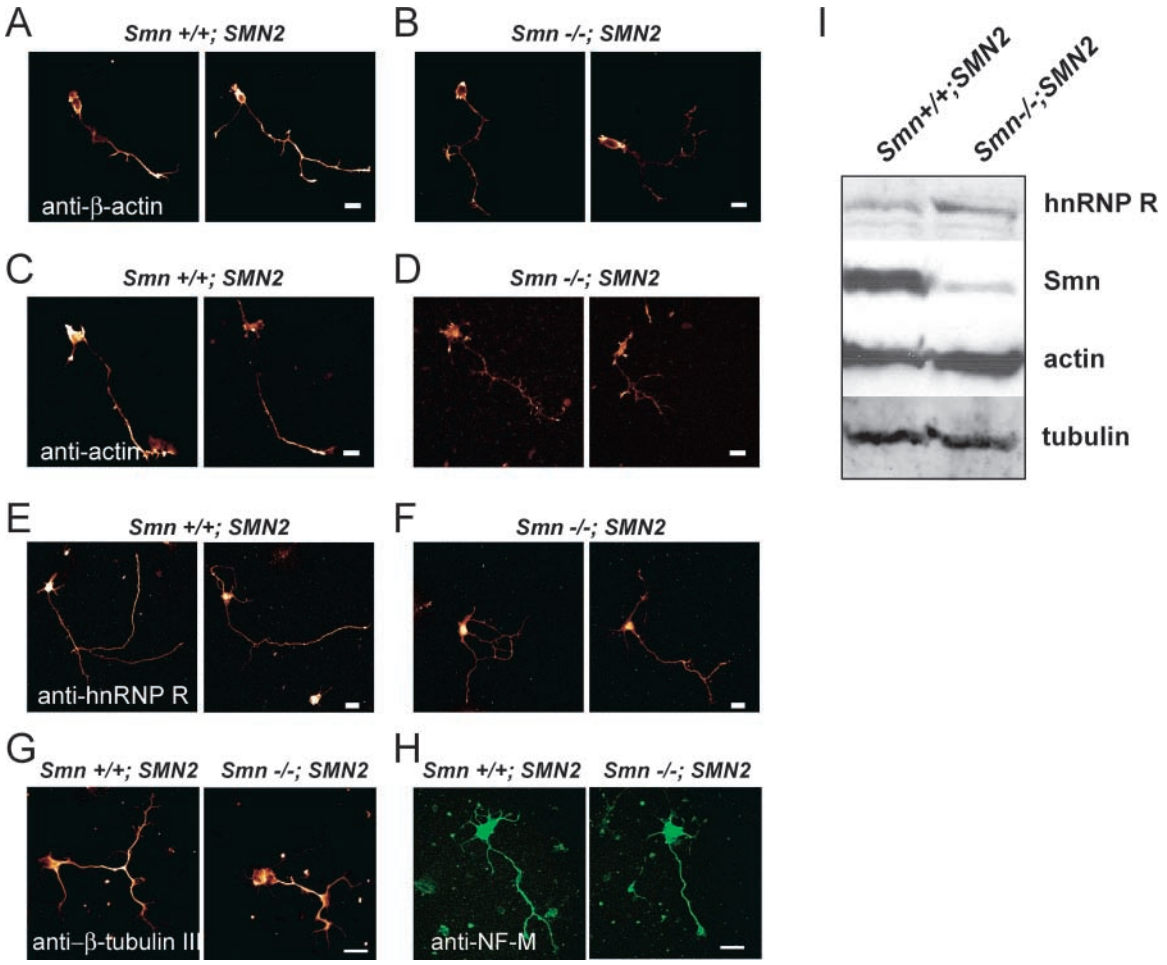


Figure 4. **Actin distribution in axons of primary cultured motoneurons from *Smn*$^{-/-}$; *SMN2* and *Smn*$^{+/+}$; *SMN2* mice.** (A and B) Motoneurons from *Smn*$^{+/+}$; *SMN2* and *Smn*$^{-/-}$; *SMN2* kept in culture for 5 d were immunostained with β-actin antibody. Motoneurons isolated from *Smn*$^{+/+}$; *SMN2* mice, but not their *Smn*$^{-/-}$; *SMN2* littermates, show strong accumulation of β-actin in distal axons and growth cones. (C and D) Immunostaining with pan-actin antibodies. *Smn*$^{+/+}$; *SMN2* motoneurons exhibit a distinct gradient from the shaft to the growth cone and an accumulation of actin in the growth cone, whereas in cells from *Smn*$^{-/-}$; *SMN2* littermates, actin staining is predominantly concentrated in cell bodies. (E and F) Immunostaining with anti-hnRNP R antiserum. Control motoneurons show strong staining in the nucleus and a distinct gradient from the shaft to the growth cone, which appears weaker in *Smn*$^{-/-}$; *SMN2* cells. (G and H) Immunostaining with anti-tubulin (β-tubulin III) and anti-neurofilament (NF-M) antibodies. There is no difference in the distribution of both cytoskeletal proteins in axons of Smn-deficient and control motoneurons. Bars, 20 μm. (I) Western blot analysis of Smn and hnRNP R in brain extracts from *Smn*$^{-/-}$; *SMN2* and control embryonic day 14 embryos. Smn protein is strongly reduced in *Smn*$^{-/-}$; *SMN2,* whereas hnRNP-R levels are not affected. The blot was subsequently stained for actin, and tubulin was used as a loading control.

staining along the neurites with an accumulation in the growth cone was reduced in Smn mutant motoneurons (Fig. 4, E and F). These results suggest that the localization of hnRNP R to axons depends on the presence of Smn. This observation correlates with our finding that hnRNP R ΔSmn is not translocated to neurites in PC12 cells, and thus accumulates within the nucleus (Fig. 2, F and G). To find out whether the total amount of hnRNP R or actin is affected, we performed Western blot analysis of Smn, hnRNP R, and actin in brain extracts from embryonic day 14 Smn-deficient and control embryos. Although Smn is severely reduced in *Smn*$^{-/-}$; *SMN2* mice, no difference was found for hnRNP R and actin (Fig. 4 I). It could be that Smn and hnRNP R are only necessary in motoneurons (and not in other neurons) for enhanced levels of β-actin in growth cones. Alternatively, the levels of β-actin and hnRNP R protein in growth cones might be so low in comparison to the levels in the cell bodies and dendrites that a specific reduction cannot be detected by Western blots of whole-brain protein extracts.

To investigate whether the distribution of other cytoskeletal proteins is also affected, we immunostained cultured motoneurons from *Smn*$^{-/-}$; *SMN2* and control mice with antibodies against tubulin (Fig. 4 G, β-tubulin III) and neurofilament (Fig. 4 H, NF-M). Both proteins were present at normal levels and distribution in the axons of cultured *Smn*$^{-/-}$; *SMN2* motoneurons.

## Reduced growth cone area in Smn-deficient motor axons

High power magnification of the distal axons stained with antibodies against β-actin, tubulin (β-tubulin III), and neurofilament (NF-M) showed a distinct reduction of growth cone size by all antibodies used (Fig. 5, A, C, and D). Staining with β-actin, which is enriched in growth cones includ-

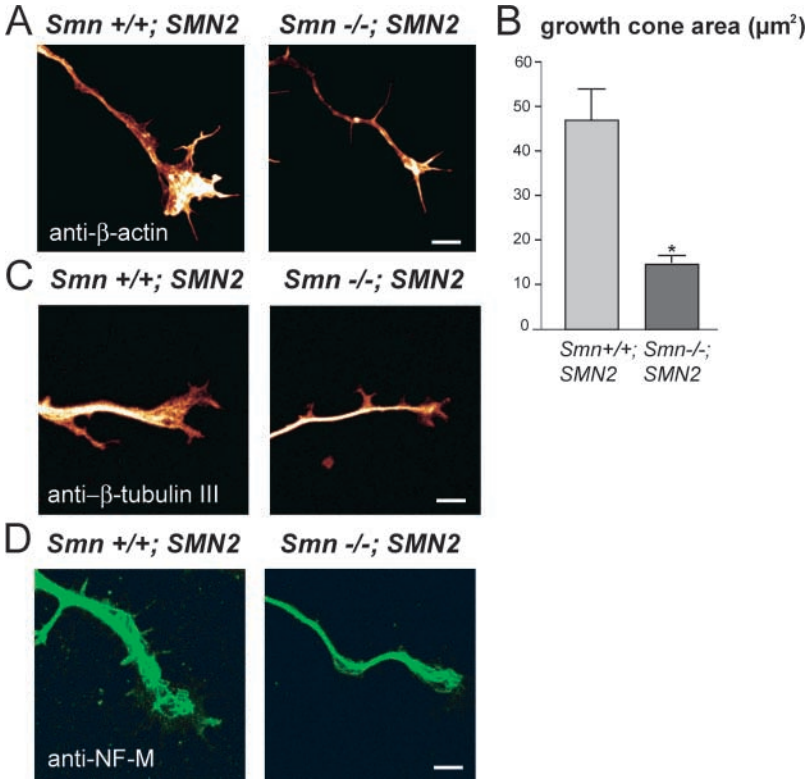


Figure 5. **Reduced growth cone size in primary cultured motoneurons from *Smn*$^{-/-}$; *SMN2* mice.** (A) High power magnification of β-actin–stained axonal growth cones in cultured *Smn*$^{+/+}$; *SMN2* motoneurons. Bar, 5 μm. (B) Motoneurons from *Smn*$^{+/+}$; *SMN2* ($n = 35$) and *Smn*$^{-/-}$; *SMN2* ($n = 31$) mice were cultured for 5 d, stained with β-actin, and the area covered by the axonal growth cone was measured. *Smn*$^{-/-}$; *SMN2* mice show a significant reduction of the average growth cone area (14.36 ± 2.07 μm$^2$ vs. 46.73 ± 6.9 μm$^2$). (C) β-Tubulin staining and (D) neurofilament (NF-M) staining of axonal growth cones in cultured motoneurons from *Smn*$^{-/-}$; *SMN2* and control mice. Bars, 5 μm.

ing the filopodia, was used for morphometric analysis. The results show a more than threefold reduction of the area covered by the axonal growth cones in *Smn*$^{-/-}$; *SMN2* motoneurons (Fig. 5 B).

## hnRNP R and Smn modulate localization of actin mRNA in neurites

It has been shown that β-actin protein accumulation in the growth cone depends to a large extent on axonal transport of β-actin mRNA (Kislauskis et al., 1997). Because hnRNP R is an RNA-binding protein (Rossoll et al., 2002), we investigated whether hnRNP R and Smn participate in this function. To localize actin mRNA, we performed in situ hybridization with an antisense probe for the coding region of β-actin. Stable PC12 cell lines overexpressing either wild-type hnRNP R, hnRNP R ΔRRM, or hnRNP R ΔSmn were differentiated with NGF for 7 d. Actin mRNA was detected with biotin-labeled actin-specific oligo probes and visualized by HRP-coupled streptavidin and DAB staining. Actin mRNA accumulates in the growth cones of full-length hnRNP R–overexpressing PC12 cells, but is hardly visible in PC12 cells overexpressing mutated hnRNP R (Fig. 6 A). A sense probe was used as a specificity control (Fig. 6 B). It is possible that the probe also detects γ-actin transcripts. However, previous works have shown that only the β isoform accumulates in distal parts of axons and in growth cones (Bassell et al., 1998). Therefore, we conclude that most of the reduction of the signal observed by in situ hybridization is due to a reduction of β-actin mRNA levels in distal motor axons. Our results suggest that hnRNP R plays a role in the translocation of β-actin transcripts to neurites, and that interaction with Smn is required for this function.

Furthermore, we analyzed the localization of β-actin mRNA in the axons of cultured *Smn*$^{+/+}$; *SMN2* and *Smn*$^{-/-}$; *SMN2* motoneurons. In situ hybridization shows reduced distal axonal localization of β-actin mRNA in Smn-deficient cells in comparison to control cells (Fig. 6 C). Quantitative analysis by visual scoring shows a significant reduction in the number of actin mRNA–positive growth cones in *Smn*$^{-/-}$; *SMN2* motoneurons (Fig. 6 E). No specific signal was obtained with the sense probe (Fig. 6 D). Our results indicate that Smn deficiency leads to reduced axonal actin mRNA levels in motoneurons.

## hnRNP R associates with the 3′ UTR of β-actin mRNA

It has been shown that the 3′ UTR of β-actin is important for the transport of the transcript (Kislauskis et al., 1993). A 54-bp domain called zipcode (Kislauskis et al., 1994) is bound by specific proteins that are involved in this process (Ross et al., 1997; Zhang et al., 2001; Gu et al., 2002). Therefore, we investigated whether hnRNP R or Smn can interact with the 3′ UTR of β-actin mRNA in vitro.

Full-length HA-tagged hnRNP R, hnRNP R ΔRRM1,2, and the hnRNP R ΔSmn mutants, as well as HA-tagged Smn and the transcription factor c-Jun (as a negative control), were immunopurified from transfected HEK 293 cells and incubated with either the full-length 3′ UTR of β-actin mRNA or the fragment corresponding to the zipcode region (Kislauskis et al., 1994). Both in vitro–transcribed RNAs contained a poly(A)$^+$ tail of 30 nucleotides. A full-length cDNA clone of IκBα including the 3′ UTR and the poly(A)$^+$ tail was used as a specificity control. The 3′ UTR of β-actin mRNA and also the truncated RNA, which consisted of only the zipcode region, was specifically

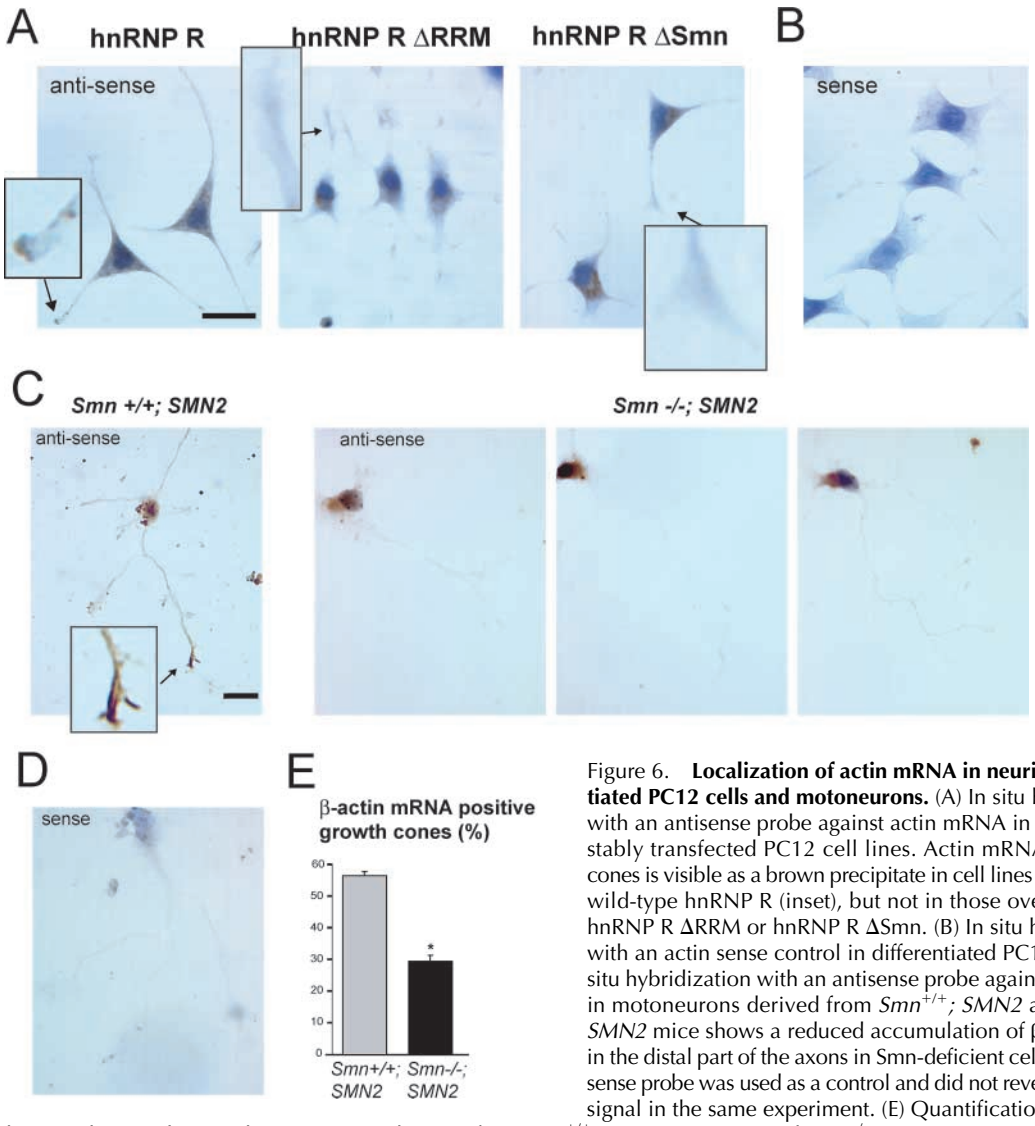


Figure 6. **Localization of actin mRNA in neurites of differentiated PC12 cells and motoneurons.** (A) In situ hybridization with an antisense probe against actin mRNA in differentiated stably transfected PC12 cell lines. Actin mRNA in growth cones is visible as a brown precipitate in cell lines overexpressing wild-type hnRNP R (inset), but not in those overexpressing hnRNP R ΔRRM or hnRNP R ΔSmn. (B) In situ hybridization with an actin sense control in differentiated PC12 cells. (C) In situ hybridization with an antisense probe against actin mRNA in motoneurons derived from *Smn*$^{+/+}$*; SMN2* and *Smn*$^{-/-}$*; SMN2* mice shows a reduced accumulation of β-actin mRNA in the distal part of the axons in Smn-deficient cells. (D) An actin sense probe was used as a control and did not reveal a detectable signal in the same experiment. (E) Quantification of the actin mRNA levels in the growth cones by visual scoring. Growth cones from *Smn*$^{+/+}$*; SMN2* ($n = 403$) and *Smn*$^{-/-}$*; SMN2* ($n = 368$) motoneurons were compared. Smn-deficient motoneurons show a significant reduction in the percentage of actin mRNA–positive growth cones ($56.25 \pm 1.493$ vs. $29.50 \pm 1.709$). Results represent the mean ± SEM of pooled data from four independent experiments. *, $P < 0.05$ between control and Smn-deficient motoneurons. Bars, 20 μm.

bound by full-length hnRNP R, but neither by the truncated hnRNP R mutants nor by Smn alone or c-Jun (Fig. 7 A). No interaction was observed between hnRNP R and IκBα mRNA (Fig. 7 A). To rule out that hnRNP R interaction specifically involves the poly(A)$^+$ tail of β-actin mRNA, we performed similar experiments using the full-length 3′ UTR of β-actin mRNA with or without a 30-mer poly(A)$^+$ tail. A 500-bp fragment of lysozyme mRNA, containing the COOH terminus of the ORF and part of the 3′ UTR, was used as a specificity control. Specific association was observed for both constructs of β-actin mRNA (Fig. 7 B). These data strongly indicate that hnRNP R interacts with the 3′ UTR of β-actin.

We also investigated whether Smn binding to hnRNP R is necessary for this effect. When hnRNP R ΔSmn was tested for interaction with β-actin mRNA, no specific association was observed (Fig. 7, A and B), although this truncated form of hnRNP R still contains the RRMs.

To show association of β-actin transcripts with hnRNP R in vivo, we performed RT-PCR of mRNA coimmunoprecipitated with hnRNP R. HA-tagged wild-type hnRNP R or the ΔRRM and ΔSmn mutants were immunopurified from differentiated PC12 cell lines. Bound mRNA was isolated from immunoprecipitates, was reverse transcribed into cDNA, and RT-PCR was performed with β-actin–specific primers. A 209-bp DNA fragment can be amplified from RNA bound to wild-type hnRNP R, but is barely visible when using RNA bound by mutant hnRNP R (Fig. 7 C). c-Jun–specific primers used as a specificity control do not amplify a DNA fragment (expected size of 213 bp). Although we can clearly show association of β-actin mRNA and hnRNP R, future work is needed to demonstrate whether this interaction is direct, or whether it involves additional proteins like ZBP1 (Zhang et al., 2001) or ZBP2 (Gu et al., 2002).

In summary, our results show that a complex of Smn and hnRNP R associates with β-actin mRNA and translocates to

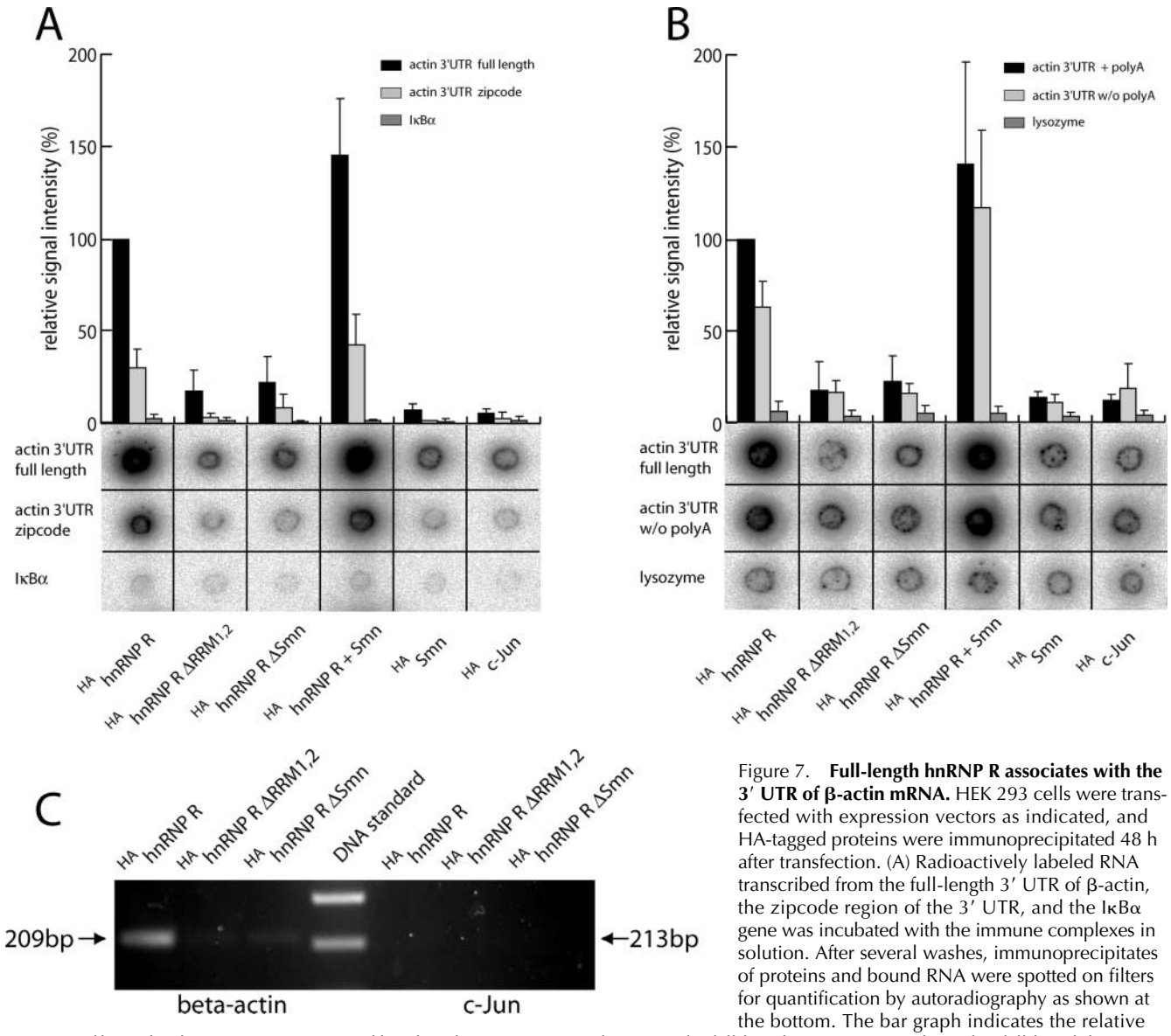


Figure 7. **Full-length hnRNP R associates with the 3′ UTR of β-actin mRNA.** HEK 293 cells were transfected with expression vectors as indicated, and HA-tagged proteins were immunoprecipitated 48 h after transfection. (A) Radioactively labeled RNA transcribed from the full-length 3′ UTR of β-actin, the zipcode region of the 3′ UTR, and the IκBα gene was incubated with the immune complexes in solution. After several washes, immunoprecipitates of proteins and bound RNA were spotted on filters for quantification by autoradiography as shown at the bottom. The bar graph indicates the relative amounts of bound radioactive RNA measured by phosphorimaging. Signal intensity for full-length β-actin 3′ UTR bound to full-length hnRNP R was set as 100%. Values are given as relative signal intensities. The full-length 3′ UTR of β-actin and also the zipcode region are bound by full-length hnRNP R, but not by mutant hnRNP R or Smn alone. (B) Radioactively labeled RNA transcribed from the full-length 3′ UTR of β-actin either with or without a poly(A)$^+$ tail and the lysozyme mRNA was incubated with the immune complexes. The graph indicates the amounts of bound radioactively labeled RNA. The 3′ UTR of β-actin both with or without a poly(A)$^+$ tail are bound by full-length hnRNP R. (C) RT-PCR of β-actin coimmunoprecipitated with hnRNP R. HA-tagged wild-type and mutant hnRNP R was immunopurified from differentiated PC12 cell lines with HA-antibody. RNA was isolated from immunoprecipitates, reverse transcribed into cDNA, and RT-PCR was performed with β-actin–specific primers (35 cycles). A clear band of 209 bp can be amplified from RNA bound to wild-type hnRNP R (contamination with genomic DNA would yield a larger fragment including an intron of 123 bp). c-Jun–specific primers were used as a specificity control (expected size of 213 bp).

axons in motoneurons. Disturbances in this process could lead to reduced β-actin levels in growth cones, and thus to reduced axon growth in SMA.

## Discussion

Despite recent progress in the understanding of the role of SMN in snRNP assembly, there is no evidence so far that disturbance of this function is responsible for the development of motoneuron disease in SMA. We define a role of Smn and its binding partner hnRNP R in axonal growth in motoneurons. Furthermore, we show that dendrite growth is not disturbed in motoneurons from Smn mutant mice. We also found that Smn deficiency had no effect on motoneuron survival in cell culture. These data suggest that disturbances in axon growth and maintenance are the primary cellular defects that ultimately may lead to loss of motoneurons in SMA. Recently, it has been shown that reduction of Smn levels in zebrafish embryos causes axon-specific pathfinding defects in motoneuron development (McWhorter et al., 2003). These data support our finding of specific axonal defects in Smn-deficient murine motoneurons.

In differentiating PC12 cells, overexpression of Smn as well as hnRNP R leads to enhanced neurite outgrowth. This effect depends on the interaction of these two proteins. They are colocalized in axons of cultured motoneurons and also in axons of motor nerves in adult mice (Rossoll et al., 2002). SMN protein has been shown to be present in a stable complex with Gemin2–7 (for review see Meister et al., 2002; Paushkin et al., 2002) in the nucleus within specific structures called gemini of Cajal (coiled) bodies ("gems"). Interestingly, hnRNP R has not been identified as part of this complex. Gems seem to play an important role for snRNP assembly and RNA processing (Carvalho et al., 1999; Young et al., 2000; Sleeman et al., 2001). In motoneurons, Smn is also localized in axons (Pagliardini et al., 2000; Jablonka et al., 2001; Fan and Simard, 2002), but it does not colocalize with Gemin2 (Jablonka et al., 2001), and instead colocalizes with hnRNP R in this part of the cell (Rossoll et al., 2002). Others have observed Smn in association with cytoskeletal elements in spinal dendrites and axons (Bechade et al., 1999; Pagliardini et al., 2000). Recently, cytoskeletal-based active transport of SMN containing granules in neuronal processes and growth cones has been demonstrated in transfected cultured neurons (Zhang et al., 2003). Binding of Smn to hnRNP R and localization of these proteins in motor axons (Rossoll et al., 2002) suggest that Smn could be involved in the transport of specific mRNAs in motor axons.

Increasing evidence points to the importance of RNA localization and transport within polarized cells. Sorting of defined mRNA species to distinct subcellular regions is observed in many cell types, in particular in neurons (for review see Mohr and Richter, 2001). The actin cytoskeleton plays an important role in axon initiation, growth, guidance, branching, and retraction, and also in synapse formation and stability (for review see Luo, 2002). β-Actin protein is highly enriched in distal parts of axons and growth cones. Specific transport of β-actin mRNA to axons contributes to this distribution (Bassell et al., 1998; Zhang et al., 1999, 2001). Our observation that axon growth is significantly impaired in *Smn*$^{-/-}$*; SMN2* motoneurons (and that β-actin protein distribution and growth cone morphology is disturbed in these cells) points to an essential role of Smn and hnRNP R in this function. To investigate a possible direct effect on the transport of β-actin mRNA, we performed in situ hybridization experiments to localize actin transcripts in neurites of developing PC12 cells and primary motoneurons (Fig. 6). Our results suggest that wild-type Smn levels are required for accumulation of actin mRNA in growth cones of motoneurons. Furthermore, we show that hnRNP R mutants that cannot bind RNA or Smn exert a dominant-negative effect on mRNA translocation. This corresponds to reduced neurite growth in PC12 cell lines that express hnRNP R ΔRRM (Fig. 3 A). Our data show that the observed reduced distal β-actin protein localization is caused, at least to some extent, by a direct effect of Smn and hnRNP R on distal actin mRNA accumulation.

It has been shown that the localization of β-actin mRNA involves a 54-nt sequence within the 3′ UTR (termed zipcode) that is both sufficient and necessary for peripheral localization (Kislauskis et al., 1994). Our findings indicate that hnRNP R can associate with full-length β-actin mRNA as well as the zipcode region, and that this interaction does not depend on a poly(A)$^+$ tail. Because neither the lysozyme nor the IκBα control mRNAs are bound, specificity for this interaction can be anticipated. Two proteins, ZBP1 and ZBP2, which interact with the same zipcode domain of β-actin mRNA and seem to be involved in axonal transport of β-actin mRNA in chick forebrain (Zhang et al., 2001; Gu et al., 2002) or rat cortical neurons (Bassell et al., 1998), have been identified. However, it is not clear so far whether these proteins need the hnRNP R–Smn complex for this effect, or whether motoneurons specifically require this complex either in concert or independently from ZBP1 and ZBP2. Many attempts have been made to identify Smn-interacting proteins (for review see Meister et al., 2002; Paushkin et al., 2002), but interaction with ZBP1 and ZBP2 has not been found by such efforts. Further experiments with mouse gene knockout models will need to show the specific requirement of ZBP1, ZBP2, and/or the hnRNP R/Q–Smn complex for axonal β-actin mRNA transport in motoneurons and other types of neurons.

It is possible that the role of hnRNP R–Smn in motoneurons goes beyond transport of β-actin mRNA. hnRNP Q has been implicated in regulation of mRNA stability (Grosset et al., 2000), editing (Blanc et al., 2001; Lau et al., 2001), and splicing (Mourelatos et al., 2001). Therefore, the precise function of these RNA-binding proteins in axons remains to be determined. For example, it could be that the interaction of β-actin mRNA and hnRNP R–Smn also controls stability of β-actin mRNA in motor growth cones. It could also be that this complex is part of a regulatory machinery that controls local actin protein translation in response to extracellular stimuli, which control growth cone migration, presynaptic differentiation, and functions at the motor endplate. This scenario appears as a tempting model to interpret the pathophysiology of SMA. Recently, it has been proposed that the primary function of actin in the growth cone is not propulsion, but is to act as a scaffold for regulatory molecules in the presynapse (Sankaranarayanan et al., 2003). Specific defects in neurofilament distribution in motor axons, as well as defects of axonal sprouting and axonal growth, were observed in another mouse model (Cifuentes-Diaz et al., 2002). Although we did not find a direct effect on the distribution of neurofilaments in axons, a relative accumulation in growth cones was observed. However, this appears as a consequence to reduced β-actin content in growth cones and reduced size of the axon terminals. In this scenario, proteins that normally are not present in presynaptic structures, such as neurofilaments and microtubules, appear more distal in growth cones. The reduced levels of actin suggest that functions such as growth cone movement and the release of synaptic vesicles (Doussau and Augustine, 2000; Bloom et al., 2003), which also require actin, might be disturbed in SMA, and thus contribute to the specific pathology of this disease. Defects in dynamic processes that are necessary for further maturation and function of the presynaptic part of the motor endplate could thus constitute a major part of the pathophysiology of SMA. Future experiments will have to show whether the hnRNP R–Smn complex also modulates synaptic excitability, and thus plays a role that goes beyond the observed effect on axon growth in motoneurons.

# Materials and methods

## DNA cloning

3HA-tagged hnRNP R and FLAG-tagged Smn were cloned as described previously (Rossoll et al., 2002). 2HA-tagged Smn was created by inserting the FLAG-tagged Smn into pcDNA3 containing two HA-tags. The truncated versions of hnRNP R were generated by a PCR-based method using PCR primers as follows: hnRNP R-HA forward, 5′-AGAGGTACCACCATGGGCTACCCCTACGACGTGCCC-3′; hnRNP R reverse, 5′-ATATCTAGACTACTTCCACTGCCCATAAGTATC-3′; hnRNP R del RRM forward, 5′-CGGGTGTGCAGCCTGGGATTGGGACAGAGTGGGCTGACCCCGTGGAGGAG-3′; hnRNP R del RRM reverse, 5′-CTGGATCCGGCTCCTCCACGGGGTCAGCCCACTCTGTCCCAATCCCAGGCT-3′; hnRNP R del Smn forward, 5′-CCACCACCACCAAGGGGGCGGGGAGCACCACCTCCATCTCGTGGAGCTCGGGGCAATCG-3′; and hnRNP R del Smn reverse 5′-GCCCCCTCGATTGCCCCGAGCTCCACGAGATGGAGGTGGTGCTCCCCGCCCCCTTG-3′. HA-tagged c-Jun was cloned by PCR from genomic DNA, and primers were as follows: HA–c-Jun forward, 5′-TATAGGTACCATGGGCTACCCCTACGACGTGCCCGACTACGCCGGCATGACTGCAAAGATGGAAACGAC-3′; c-Jun reverse, 5′-TGAGCAGCCCGACGTCGGGCGCCGTGAGAAGGTCCGAGTTC-3′.

The entire 3′ UTR of murine β-actin cDNA as well as a fragment containing the putative zipcode region (Kislauskis et al., 1994) including a poly(A)$^+$ tail of 30 nucleotides were cloned by RT-PCR into pTZ19, and primers were as follows: actinUTR forward, 5′-ATGAAAGCTTAGGCGGACTGTTACTGAGCTGC-3′; actinUTRpolyAfull reverse, 5′-ATGAGAATTC-T$_{(30)}$-GTGTAAGGTAAGGTGTGCAC-3′; actinUTRpolyAzip reverse, 5′-ATGAGAATTC-T$_{(30)}$-CTGCGCAAGTTAGGTTTTGTC-3′; and actin UTRfull reverse, 5′-ATGAGGATCCGTGTAAGGTAAGGTGTGCAC-3′. For RT-PCR of rat β-actin and c-Jun from PC12 cells, primers were used as follows: Rn actinup, 5′-AAGACCTCTATGCCAACACAG-3′; Rn actinlow, 5′-CTGCTTGCTGATCCACATCTG-3′; RncJunup, 5′-AGCGCATGAGAAACCGCATCG-3′; and RncJunlow, 5′-TGCAACTGCTGCGTTAGCATG-3′. PCR reactions were performed under standard conditions using BioTherm™ polymerase (GeneCraft, Ltd.) in the presence of 1 M betaine (Sigma-Aldrich).

## PC12 culture and transfections

PC12 cells were routinely maintained in DME plus 10% horse serum, 5% FCS, and antibiotics (Invitrogen). For transfection experiments, the cells were plated at high density in 24-well plates and transfected with 1 μg plasmid DNA (empty vector and/or hnRNP R constructs and/or Smn constructs, to keep the total DNA amount constant) using LipofectAMINE™ 2000 (Invitrogen) according to the manufacturer's instructions. The day after transfection, cells were replated in 35-mm dishes containing poly-DL-ornithine–coated glass coverslips at a 1,000-cells/cm$^2$ density in DME plus 2% horse serum, 1% FCS, antibiotics, and 50 ng/ml NGF to stimulate neurite outgrowth. After 3 d of NGF treatment, the cells were fixed and stained as described below.

To establish stable cell lines, transfected PC12 cells were selected for resistance to G418, and individual clones were tested for stable expression by Western blot analysis with anti-HA antibody. To assess neurite length, cells were plated as described above and treated with 50 ng/ml NGF for 7 d. Three independent cell lines for each expression vector were used.

## Motoneuron culture

Isolation and culture of embryonic motoneurons and genotyping of the individual embryos were performed as described previously (Wiese et al., 1999, 2001; Monani et al., 2000).

## Immunocytochemistry

Motoneurons grown for 5 d on glass coverslips were fixed with PFA and subsequently with acetone. After blocking with 10% BSA, the cells were incubated overnight at 4°C with primary antibodies as follows: rabbit antibodies against 1 μg/ml phospho-tau (1 μg/ml; Sigma-Aldrich) and NF-M (1:500; Abcam), a mouse mAb against MAP-2 antibody (1:1,000; CHEMICON International), actin (1:200; Roche), β-actin (1:1,000; Abcam), β-tubulin III (1:200; Research Diagnostics, Inc.), and Smn (1:1,000; Transduction Laboratories). Cells were then washed three times with TBS-T (20 mM Tris-HCl, pH 7.6, 137 mM NaCl, and 0.1% Tween 20) and incubated for 1 h at RT with Cy2- and Cy3-conjugated secondary antibodies (1:200; Dianova). After washing with TBS-T, coverslips were embedded in Mowiol.

PC12 cells were fixed with 4% PFA and blocked with 15% normal goat serum plus 0.3% Triton X-100 in PBS, and were incubated overnight at 4°C with antibodies as follows: anti-neurofilament H (1:400; Sigma-Aldrich), rabbit antibodies against hnRNP R (1:100; Rossoll et al., 2002), monoclonal anti-HA (HA.11, 1:250; Covance), monoclonal anti-FLAG M2 (1:500; Sigma-Aldrich), and monoclonal anti-Smn (1:500; BD Biosciences). Cells were then washed, incubated with secondary antibodies, and embedded as described in the previous paragraph. Immunoreactivity was visualized with a confocal microscope (Leica), with identical settings for pinhole and voltage for any panel of analysis.

## In situ hybridization

Cells grown on glass coverslips were fixed with 4% PFA in PBS for 15 min at RT, and were then washed with PBS containing 0.1% active diethyl pyrocarbonate for 10 min at RT. Cells were then permeabilized with 0.3% vol/vol Triton X-100 in PBS for 20 min at RT, and endogenous peroxidase activity was quenched through incubation in 0.3% vol/vol $H_2O_2$ in methanol for 40 min at RT. Prehybridization, hybridization, and washes were performed according to the manufacturer's instructions (GeneDetect). Oligonucleotide probes (3′ biotinylated) were applied to the coverslips at 200 ng/ml (antisense, 5′-GCCGATCCACACGGAGTACTTGCGCTCAGGAGGAGCAATGATCTTGAT-3′; sense control, 5′-CGGCTAGGTGTGCCTCATGAACGCGAGTCCTCCTCGTTACTAGAACTA-3′; GeneDetect).

Hybridized probe was detected through a tyramide signal amplification system (GenPoint; DakoCytomation) according to the manufacturer's instructions. Finally, coverslips were counterstained with hematoxylin, dehydrated, and mounted with VitroClud (Legenbrick). Images were acquired with a microscope (Axiophot; Leica) equipped with a CCD camera using Axioplan 2 software (Leica). Growth cones were visually scored for the absence or presence of actin mRNA signal. Multiple scoring of the same growth cones was avoided by recording the position of the cells.

## Western blot analysis

Western blot analysis was performed as described previously (Rossoll et al., 2002). The primary antibodies were used at a dilution of 1:1,000 each: hnRNP R (Rossoll et al., 2002), Smn (Transduction Laboratories), actin (Roche), and β-tubulin (CHEMICON International).

## Data analysis

For the quantification of neurite length and growth cone area, only motoneurons that allowed a clear distinction between axons and dendrites were scored. Axons were identified as phospho-tau–positive processes that are at least two times longer than the phospho-tau–negative dendrites. Both the longest axonal branches and the total length of all axonal branches were measured. Cultures obtained from four mutant and control embryos ($n = 4$) from different litters were scored.

In NGF-treated PC12 cells, axons and dendrites cannot be distinguished. Therefore, all neurites were measured and the average of the three longest processes was calculated. For transient transfection of PC12 cells, at least 30 cells were analyzed per treatment group and four independent experiments were performed. Only transfected cells as shown by staining with the HA antibody (hnRNP R constructs) or FLAG antibody (Smn constructs) were scored. For the stable cell lines, the average length of all neurites was calculated and data were collected from three independent cell lines for each group. Images recorded at the confocal microscope were analyzed using the Scion Image software package (Scion Corporation). Data were analyzed using the *t* test.

## mRNA binding assay

β-Actin clones were linearized at the 3′ end with EcoRI, purified, and 0.2 μg was used for in vitro transcription with T7 RNA polymerase (T7 Transcription Kit; MBI Fermentas) in the presence of α[$^{32}$P]CTP. A 500-bp fragment of the chicken lysozyme gene (included in the kit) and a full-length clone of IκBα cDNA were used as specificity controls. Labeled RNA was purified on G-25 columns (Amersham Biosciences) and radioactive counts were measured for standardization. HEK293 cells were transfected with HA-tagged constructs of hnRNP R, Smn, and c-Jun (LipofectAMINE™ 2000; Invitrogen). DNA concentration was kept constant by adding empty vector. 48 h after transfection, cells were lysed in IP buffer (25 mM Tris-HCl, pH 8.0, 137 mM NaCl, 2 mM EGTA, 2 mM EDTA, 10% glycerol, 1% Triton X-100, 0.05% 2-mercaptoethanol, and protease inhibitors; Roche), and HA-tagged proteins were immunopurified by overnight incubation with HA beads (HA.11; Covance). The immunoprecipitate was washed 5× with IP-buffer and 1× with RNA-binding buffer (RBB; 10 mM Tris, pH 7.5, 1.5 mM $MgCl_2$, 250 mM KCl, 2 mM DTT, and 0.25% Triton X-100). Immunoprecipitates were incubated with labeled RNA probes in RBB for 30 min at RT. The RNA-bound immune complexes were washed three times with RBB and RBB plus 5 mg/ml heparin (Sigma-Aldrich). For quantifications, the pellets were resuspended in 20 μl RBB, spotted on nitrocellulose membranes, and exposed to image plates (BAS 2500; Fuji). Bound radioactivity

was quantified as photostimulated luminescence/spot area with the AIDA software package (Raytest). Experiments were repeated at least three times, and typical results are shown. Signal intensity for full-length β-actin 3′ UTR bound to full-length hnRNP R was defined as 100% in each experiment. All values were calculated as relative signal intensities.

For RT-PCR of hnRNP R–associated β-actin, HA-tagged wild-type and mutant hnRNP R were immunoprecipitated from differentiated PC12 cell lines with HA antibody. Cells were lysed in RBB containing 100 U/ml RNase inhibitor (Superasin; Ambion) and protease inhibitor (Roche), and were incubated with HA beads (HA.11; Covance) for 30 min at 4°C. Beads were washed 5× with RBB, the pellet was resuspended in 500 μl TRIzol® (Invitrogen), and 100 μg glycogen (Roche) was added. RNA was isolated from immunoprecipitates according to the manufacturer's instructions and was reverse transcribed into cDNA using oligo dT primers (SuperScript™ first strand synthesis system; Invitrogen). RT-PCR was performed with β-actin–specific primers with 25–35 cycles (15 s at 94°C; 15 s at 57°C; 30 s at 72°C). These primers amplify a DNA fragment of 209 bp. Contamination with rat genomic DNA would yield a larger fragment, including an intron of 123 bp. c-Jun–specific primers that were able to amplify a 213-bp fragment from rat cDNA were used as a specificity control.

### Online supplemental material

Fig. S1 shows immunolocalization of Smn in PC12 cell lines. The online supplemental material is available at http://www.jcb.org/cgi/content/full/jcb.200304128/DC1.

We thank Stephanie Renninger, Beate Christ, and Christine Schneider for technical assistance, and Stefan Wiese for help in establishing the setup for measuring axon and dendrite length in cultured motoneurons.

This work was supported by the Schilling Stiftund and by the Deutsche Forschungsgemeinschaft, SFB 581 TP B1 and B4. M. Sendtner is the recipient of support from the Initiative Forschung und Therapie für die SMA. Umrao Monani is a recipient of a Development Grant from the Muscular Dystrophy Association of America.

Submitted: 23 April 2003
Accepted: 1 October 2003

## References

Bassell, G.J., H. Zhang, A.L. Byrd, A.M. Femino, R.H. Singer, K.L. Taneja, L.M. Lifshitz, I.M. Herman, and K.S. Kosik. 1998. Sorting of β-actin mRNA and protein to neurites and growth cones in culture. *J. Neurosci.* 18:251–265.

Bechade, C., P. Rostaing, C. Cisterni, R. Kalisch, V. La Bella, B. Pettmann, and A. Triller. 1999. Subcellular distribution of survival motor neuron (SMN) protein: possible involvement in nucleocytoplasmic and dendritic transport. *Eur. J. Neurosci.* 11:293–304.

Blanc, V., N. Navaratnam, J.O. Henderson, S. Anant, S. Kennedy, A. Jarmuz, J. Scott, and N.O. Davidson. 2001. Identification of GRY-RBP as an apolipoprotein B RNA-binding protein that interacts with both apobec-1 and apobec-1 complementation factor to modulate C to U editing. *J. Biol. Chem.* 276:10272–10283.

Bloom, O., E. Evergren, N. Tomilin, O. Kjaerulff, P. Low, L. Brodin, V.A. Pieribone, P. Greengard, and O. Shupliakov. 2003. Colocalization of synapsin and actin during synaptic vesicle recycling. *J. Cell Biol.* 161:737–747.

Bommel, H., G. Xie, W. Rossoll, S. Wiese, S. Jablonka, T. Boehm, and M. Sendtner. 2002. Missense mutation in the tubulin-specific chaperone E (Tbce) gene in the mouse mutant progressive motor neuronopathy, a model of human motoneuron disease. *J. Cell Biol.* 159:563–569.

Carvalho, T., F. Almeida, A. Calapez, M. Lafarga, M.T. Berciano, and M. Carmo-Fonseca. 1999. The spinal muscular atrophy disease gene product, SMN: A link between snRNP biogenesis and the Cajal (coiled) body. *J. Cell Biol.* 147:715–728.

Cifuentes-Diaz, C., S. Nicole, M.E. Velasco, C. Borra-Cebrian, C. Panozzo, T. Frugier, G. Millet, N. Roblot, V. Joshi, and J. Melki. 2002. Neurofilament accumulation at the motor endplate and lack of axonal sprouting in a spinal muscular atrophy mouse model. *Hum. Mol. Genet.* 11:1439–1447.

Doussau, F., and G.J. Augustine. 2000. The actin cytoskeleton and neurotransmitter release: an overview. *Biochimie.* 82:353–363.

Fan, L., and L.R. Simard. 2002. Survival motor neuron (SMN) protein: role in neurite outgrowth and neuromuscular maturation during neuronal differentiation and development. *Hum. Mol. Genet.* 11:1605–1614.

Fischer, U., Q. Liu, and G. Dreyfuss. 1997. The SMN-SIP1 complex has an essential role in spliceosomal snRNP biogenesis. *Cell.* 90:1023–1029.

Frugier, T., F.D. Tiziano, C. Cifuentes-Diaz, P. Miniou, N. Roblot, A. Dierich, M. Le Meur, and J. Melki. 2000. Nuclear targeting defect of SMN lacking the C-terminus in a mouse model of spinal muscular atrophy. *Hum. Mol. Genet.* 9:849–858.

Grosset, C., C.Y. Chen, N. Xu, N. Sonenberg, H. Jacquemin-Sablon, and A.B. Shyu. 2000. A mechanism for translationally coupled mRNA turnover: interaction between the poly(A) tail and a *c-fos* RNA coding determinant via a protein complex. *Cell.* 103:29–40.

Gu, W., F. Pan, H. Zhang, G.J. Bassell, and R.H. Singer. 2002. A predominantly nuclear protein affecting cytoplasmic localization of β-actin mRNA in fibroblasts and neurons. *J. Cell Biol.* 156:41–51.

Hadano, S., C.K. Hand, H. Osuga, Y. Yanagisawa, A. Otomo, R.S. Devon, N. Miyamoto, J. Showguchi-Miyata, Y. Okada, R. Singaraja, et al. 2001. A gene encoding a putative GTPase regulator is mutated in familial amyotrophic lateral sclerosis 2. *Nat. Genet.* 29:166–173.

Hsieh-Li, H.M., J.G. Chang, Y.J. Jong, M.H. Wu, N.M. Wang, C.H. Tsai, and H. Li. 2000. A mouse model for spinal muscular atrophy. *Nat. Genet.* 24:66–70.

Jablonka, S., B. Schrank, M. Kralewski, W. Rossoll, and M. Sendtner. 2000. Reduced survival motor neuron (*Smn*) gene dose in mice leads to motor neuron degeneration: an animal model for spinal muscular atrophy type III. *Hum. Mol. Genet.* 9:341–346.

Jablonka, S., M. Bandilla, S. Wiese, D. Buhler, B. Wirth, M. Sendtner, and U. Fischer. 2001. Co-regulation of survival of motor neuron (SMN) protein and its interactor SIP1 during development and in spinal muscular atrophy. *Hum. Mol. Genet.* 10:497–505.

Kislauskis, E.H., Z. Li, R.H. Singer, and K.L. Taneja. 1993. Isoform-specific 3′-untranslated sequences sort α-cardiac and β-cytoplasmic actin messenger RNAs to different cytoplasmic compartments. *J. Cell Biol.* 123:165–172.

Kislauskis, E.H., X. Zhu, and R.H. Singer. 1994. Sequences responsible for intracellular localization of β-actin messenger RNA also affect cell phenotype. *J. Cell Biol.* 127:441–451.

Kislauskis, E.H., X. Zhu, and R.H. Singer. 1997. β-Actin messenger RNA localization and protein synthesis augment cell motility. *J. Cell Biol.* 136:1263–1270.

Lau, P.P., B.H. Chang, and L. Chan. 2001. Two-hybrid cloning identifies an RNA-binding protein, GRY-RBP, as a component of apobec-1 editosome. *Biochem. Biophys. Res. Commun.* 282:977–983.

Lefebvre, S., L. Burglen, S. Reboullet, O. Clermont, P. Burlet, L. Viollet, B. Benichou, C. Cruaud, P. Millasseau, M. Zeviani, et al. 1995. Identification and characterization of a spinal muscular atrophy-determining gene. *Cell.* 80:155–165.

Lorson, C.L., E. Hahnen, E.J. Androphy, and B. Wirth. 1999. A single nucleotide in the SMN gene regulates splicing and is responsible for spinal muscular atrophy. *Proc. Natl. Acad. Sci. USA.* 96:6307–6311.

Luo, L. 2002. Actin cytoskeleton regulation in neuronal morphogenesis and structural plasticity. *Annu. Rev. Cell Dev. Biol.* 18:601–635.

Martin, N., J. Jaubert, P. Gounon, E. Salido, G. Haase, M. Szatanik, and J.L. Guenet. 2002. A missense mutation in Tbce causes progressive motor neuronopathy in mice. *Nat. Genet.* 32:443–447.

McWhorter, M.L., U.R. Monani, A.H. Burghes, and C.E. Beattie. 2003. Knockdown of the survival motor neuron (Smn) protein in zebrafish causes defects in motor axon outgrowth and pathfinding. *J. Cell Biol.* 162:919–932.

Meister, G., C. Eggert, and U. Fischer. 2002. SMN-mediated assembly of RNPs: a complex story. *Trends Cell Biol.* 12:472–478.

Mohr, E., and D. Richter. 2001. Messenger RNA on the move: implications for cell polarity. *Int. J. Biochem. Cell Biol.* 33:669–679.

Monani, U.R., C.L. Lorson, D.W. Parsons, T.W. Prior, E.J. Androphy, A.H. Burghes, and J.D. McPherson. 1999. A single nucleotide difference that alters splicing patterns distinguishes the SMA gene SMN1 from the copy gene SMN2. *Hum. Mol. Genet.* 8:1177–1183.

Monani, U.R., M. Sendtner, D.D. Coovert, D.W. Parsons, C. Andreassi, T.T. Le, S. Jablonka, B. Schrank, W. Rossol, T.W. Prior, et al. 2000. The human centromeric survival motor neuron gene (*SMN2*) rescues embryonic lethality in $Smn^{-/-}$ mice and results in a mouse with spinal muscular atrophy. *Hum. Mol. Genet.* 9:333–339.

Monani, U.R., M.T. Pastore, T.O. Gavrilina, S. Jablonka, T.T. Le, C. Andreassi, J.M. DiCocco, C. Lorson, E.J. Androphy, M. Sendtner, et al. 2003. A transgene carrying an A2G missense mutation in the SMN gene modulates phenotypic severity in mice with severe (type I) spinal muscular atrophy. *J. Cell Biol.* 160:41–52.

Mourelatos, Z., L. Abel, J. Yong, N. Kataoka, and G. Dreyfuss. 2001. SMN interacts with a novel family of hnRNP and spliceosomal proteins. *EMBO J.* 20:

5443–5452.

Pagliardini, S., A. Giavazzi, V. Setola, C. Lizier, M. Di Luca, S. DeBiasi, and G. Battaglia. 2000. Subcellular localization and axonal transport of the survival motor neuron (SMN) protein in the developing rat spinal cord. *Hum. Mol. Genet.* 9:47–56.

Paushkin, S., A.K. Gubitz, S. Massenet, and G. Dreyfuss. 2002. The SMN complex, an assemblyosome of ribonucleoproteins. *Curr. Opin. Cell Biol.* 14: 305–312.

Rochette, C.F., L.C. Surh, P.N. Ray, P.E. McAndrew, T.W. Prior, A.H. Burghes, M. Vanasse, and L.R. Simard. 1997. Molecular diagnosis of non-deletion SMA patients using quantitative PCR of SMN exon 7. *Neurogenetics.* 1:141–147.

Ross, A.F., Y. Oleynikov, E.H. Kislauskis, K.L. Taneja, and R.H. Singer. 1997. Characterization of a β-actin mRNA zipcode-binding protein. *Mol. Cell. Biol.* 17:2158–2165.

Rossoll, W., A.K. Kroning, U.M. Ohndorf, C. Steegborn, S. Jablonka, and M. Sendtner. 2002. Specific interaction of Smn, the spinal muscular atrophy determining gene product, with hnRNP-R and gry-rbp/hnRNP-Q: a role for Smn in RNA processing in motor axons? *Hum. Mol. Genet.* 11:93–105.

Sankaranarayanan, S., P.P. Atluri, and T.A. Ryan. 2003. Actin has a molecular scaffolding, not propulsive, role in presynaptic function. *Nat. Neurosci.* 6:127–135.

Schrank, B., R. Gotz, J.M. Gunnersen, J.M. Ure, K.V. Toyka, A.G. Smith, and M. Sendtner. 1997. Inactivation of the survival motor neuron gene, a candidate gene for human spinal muscular atrophy, leads to massive cell death in early mouse embryos. *Proc. Natl. Acad. Sci. USA.* 94:9920–9925.

Sendtner, M. 2001. Molecular mechanisms in spinal muscular atrophy: models and perspectives. *Curr. Opin. Neurol.* 14:629–634.

Sleeman, J.E., P. Ajuh, and A.I. Lamond. 2001. snRNP protein expression enhances the formation of Cajal bodies containing p80-coilin and SMN. *J. Cell Sci.* 114:4407–4419.

Wiese, S., F. Metzger, B. Holtmann, and M. Sendtner. 1999. The role of p75NTR in modulating neurotrophin survival effects in developing motoneurons. *Eur. J. Neurosci.* 11:1668–1676.

Wiese, S., G. Pei, C. Karch, J. Troppmair, B. Holtmann, U.R. Rapp, and M. Sendtner. 2001. Specific function of B-Raf in mediating survival of embryonic motoneurons and sensory neurons. *Nat. Neurosci.* 4:137–142.

Yang, Y., A. Hentati, H.X. Deng, O. Dabbagh, T. Sasaki, M. Hirano, W.Y. Hung, K. Ouahchi, J. Yan, A.C. Azim, et al. 2001. The gene encoding alsin, a protein with three guanine-nucleotide exchange factor domains, is mutated in a form of recessive amyotrophic lateral sclerosis. *Nat. Genet.* 29:160–165.

Yonekawa, Y., A. Harada, Y. Okada, T. Funakoshi, Y. Kanai, Y. Takei, S. Terada, T. Noda, and N. Hirokawa. 1998. Defect in synaptic vesicle precursor transport and neuronal cell death in KIF1A motor protein-deficient mice. *J. Cell Biol.* 141:431–441.

Young, P.J., T.T. Le, N. thi Man, A.H. Burghes, and G.E. Morris. 2000. The relationship between SMN, the spinal muscular atrophy protein, and nuclear coiled bodies in differentiated tissues and cultured cells. *Exp. Cell Res.* 256: 365–374.

Zhang, H.L., R.H. Singer, and G.J. Bassell. 1999. Neurotrophin regulation of β-actin mRNA and protein localization within growth cones. *J. Cell Biol.* 147:59–70.

Zhang, H.L., T. Eom, Y. Oleynikov, S.M. Shenoy, D.A. Liebelt, J.B. Dictenberg, R.H. Singer, and G.J. Bassell. 2001. Neurotrophin-induced transport of a β-actin mRNP complex increases β-actin levels and stimulates growth cone motility. *Neuron.* 31:261–275.

Zhang, H.L., F. Pan, D. Hong, S.M. Shenoy, R.H. Singer, and G.J. Bassell. 2003. Active transport of the survival motor neuron protein and the role of exon-7 in cytoplasmic localization. *J. Neurosci.* 23:6627–6637.